Quantum chemical study of gas-phase reactions of trimethylaluminium and triethylaluminium with ammonia in III-V nitride semiconductor crystal growth

4 **AUTHORS**, INCLUDING:

Koh Matsumoto

442 PUBLICATIONS **5,988** CITATIONS

SEE PROFILE

Quantum chemical study of gas-phase reactions of trimethylaluminium and triethylaluminium with ammonia in III–V nitride semiconductor crystal growth

Masahito Ikenaga[a], Koichi Nakamura[a], Akitomo Tachibana[a],*, Koh Matsumoto[b]

[a] *Department of Engineering Physics and Mechanics, Kyoto University, Kyoto 606-8501, Japan*
[b] *Nippon Sanso Corporation, Tsukuba Laboratory, Tsukuba 300-2611, Japan*

Abstract

We have discussed the gas-phase parasitic reactions in $MR_3/H_2/NH_3$ (M = Al, Ga, In; R = CH_3, C_2H_5) systems following the elimination of methane or ethane in terms of the regional density functional theory by carrying out ab initio quantum chemical calculations. It is clearly shown that Al source gases enhance reactivity for both of R = CH_3 and C_2H_5. Furthermore, the difference in reactivity between $M(CH_3)_3/H_2/NH_3$ and $M(C_2H_5)_3/H_2/NH_3$ systems is discussed. We found that the substitution of ethyl groups for methyl in metal source strengthens the M–N coordination interaction, and the tendency to reduce activation energies of the elimination reaction is observed. However, the steric repulsion between ethyl groups and ammonia, which hardly takes place for R = CH_3, raises activation energies in the presence of excess ammonia. © 2002 Elsevier Science B.V. All rights reserved.

PACS: 82.33.Ya; 81.05.Ea; 31.15.Ar; 31.15.Ew

Keywords: A1. Computer simulation; A1. Regional density functional theory; A3. Parasitic reactions; B1. Gallium compounds; B1. Nitrides; B2. Semiconducting III–V materials

1. Introduction

Wide-band-gap III–V nitride semiconductors attract much attention for application to blue light emitting diodes (LED) and laser diodes (LD) [1,2]. Rapid progress in the metal-organic vapour phase epitaxy (MOVPE) method makes it possible to grow GaN and InGaN crystals in atmospheric pressure [1–8]. On the other hand, the growth of AlGaN layers in atmospheric-pressure MOVPE is suppressed by gas-phase reactions among precursors leading to adduct formation, called "parasitic reactions" [3–5]. We have studied the mechanism of gas-phase reactions of trimethylaluminium (TMA), trimethylgallium (TMG), trimethylindium (TMI), and ammonia by quantum chemical approach, and have shown that TMA and its derivatives enhance reactivity to the parasitic reactions [9–14]. In order to suppress the parasitic reactions, we have to consider another Al source gas for the growth of AlGaN. Particularly, the substitute for TMA by changing alkyl groups is important because of simplicity. In this paper, we

*Corresponding author. Tel./fax: + 81-75-753-5184.
E-mail address: akitomo@scl.kyoto-u.ac.jp (A. Tachibana).

have investigated the reaction mechanism of the parasitic reactions in $MR_3/H_2/NH_3$ (M = Al, Ga, In; R = CH_3, C_2H_5) gas-phase systems following the elimination of RH molecules by carrying out ab initio quantum chemical calculations. We shall discuss in detail the effect of employing $M(C_2H_5)_3$ as the metal source in place of $M(CH_3)_3$ on the reactivity of parasitic reactions.

2. Computational methods and basis sets

Ab initio quantum chemical calculations were performed with the molecular regional (MR) DFT program package [15]. The geometries of model reaction species and transition states (TSs) were optimized by using the Lee–Yang–Parr functional [16] with the Becke's three hybrid parameter (B3LYP) [17]. We adopted the LanL2DZ* basis set: double-zeta basis set with Hay–Wadt's effective core potential (ECP) [18,19] on the metal atoms and the Dunning–Huzinaga's full double-zeta basis set [20] on the other atoms with polarization functions [21]. Analytical vibrational frequencies were obtained to calculate zero-point energy correction. The bond orders were obtained by Meyer's method [22].

3. Results and discussion

3.1. Coordination interaction between MR_3 and NH_3

In $MR_3/H_2/NH_3$ systems, Both of $M(CH_3)_3$ molecule (**1**; each one, respectively, denotes **1a**, **1g**, and **1i** for M = Al, Ga, and In, and so forth) and $M(C_2H_5)_3$ molecule (**1′**; a prime denotes ethyl species in $M(C_2H_5)_3/H_2/NH_3$ systems) make a very stable complex with ammonia, $(CH_3)_3M \cdot NH_3$ (**2**) and $(C_2H_5)_3M \cdot NH_3$ (**2′**), respectively, due to the M–N coordinate bond:

$$MR_3(\mathbf{1}/\mathbf{1'}) + NH_3 \rightarrow R_3M \cdot NH_3 \ (\mathbf{2}/\mathbf{2'}). \qquad (1)$$

The optimized M–N distances and bond orders, stabilization energies, and Mulliken charge transfer for the formation of **2/2′** are shown in Table 1. Stabilization energy is so large that even a stable $[AlR_3]_2$ dimer, whose stabilization energy are -10.15 kcal/mol for R = CH_3 and -4.32 kcal/mol for R = C_2H_5 respectively, dissociates immediately by forming **2/2′** as a form of AlR_3 monomer [12]. For R = C_2H_5, the stabilization energy and M–N bond order in **2′** are the largest in the $Al(C_2H_5)_3 + NH_3$ system, similarly as the system of R = CH_3. It is found that M–N bond orders and quantities of Mulliken charge transfer from NH_3 to MR_3

Table 1

Stabilization energy (kcal/mol), bond length (Å), and Mulliken population analysis of $(CH_3)_3M \cdot NH_3$ complex formation
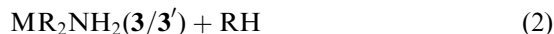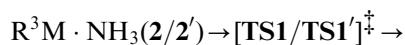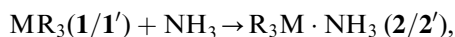
	R = CH_3			C_2H_5		
	M = Al	Ga	In	Al	Ga	In
Stabilization energy	−20.23	−16.18	−16.08	−18.99	−14.25	−14.30
Bond length of M–N in **2**	2.132	2.195	2.396	2.131	2.196	2.403
Bond order	0.337	0.287	0.194	0.401	0.317	0.209
Mulliken charge transfer						
For $NH_3 \Rightarrow \mathbf{1}$ in **2**	0.179	0.179	0.128	0.221	0.197	0.138
Atomic charge in **1**						
M	0.962	0.869	1.054	0.821	0.781	0.939
R part	−0.321	−0.290	−0.352	−0.274	−0.260	−0.313
Atomic charge in **2**						
M	1.008	0.878	1.112	0.814	0.723	0.964
R part	−0.396	−0.352	−0.414	−0.345	−0.307	−0.368
N	−0.943	−0.925	−0.966	−0.954	−0.994	−0.980
Amino-H	0.374	0.368	0.365	0.392	0.380	0.373

increase, respectively, by replacing methyl groups with ethyl groups though the optimized M–N distances of **2′** are almost equal to those of **2** for each M. According to the regional density functional theory [23–27], the electron drop region R_D, where the kinetic energy density $n_T(\mathbf{r})$ is positive [27], of $Al(C_2H_5)_3$ connects with that of NH_3 earlier in the process of complex formation than that of $Al(CH_3)_3$, as shown in Fig. 1. The arrows represent the tension density $\vec{\tau}^S(\mathbf{r})$ [27]. Connection between two R_D's means that electron in one R_D can transfer classically to the other R_D. Therefore, it is considered that the employment of $M(C_2H_5)_3$ source in substitution for $M(CH_3)_3$ could build up the M–N coordination interaction. This electronic driving force is clearly confirmed by $\vec{\tau}^S(\mathbf{r})$. The stabilization energies for the formation of complex **2′** are small to those of complex **2** for each M. This decrease in the stabilization energies is caused by the steric repulsive effect: planar coordination of metal in MR_3 molecule makes little interference between alkyl groups, but tetrahedral coordination of metal in $R_3M \cdot NH_3$, particularly for bulky R groups, destabilizes complex by gathering three alkyl groups.

3.2. RH elimination by unimolecular mechanism in $MR_3/H_2/NH_3$ system

We have investigated the reaction mechanism of the methane elimination in $M(CH_3)_3/H_2/NH_3$

systems [9–13]. Here, we shall discuss the reaction mechanism of the ethane elimination in $M(C_2H_5)_3/H_2/NH_3$ systems in addition. The *unimolecular mechanism* is represented as follows:

$$MR_3(\mathbf{1/1′}) + NH_3 \rightarrow R_3M \cdot NH_3 \, (\mathbf{2/2′}),$$

$$R^3M \cdot NH_3(\mathbf{2/2′}) \rightarrow [\mathbf{TS1/TS1′}]^{\ddagger} \rightarrow$$
$$MR_2NH_2(\mathbf{3/3′}) + RH \qquad (2)$$

for $R = CH_3/C_2H_5$. The optimized structure of **TS1a′** is shown in Fig. 2, and the relative energies of reaction species are shown in Table 2. We have
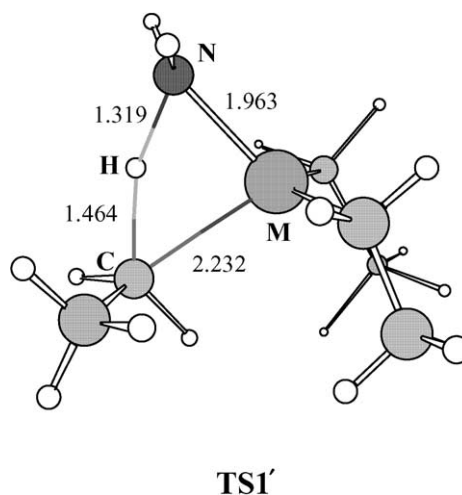

Fig. 2. B3LYP/LanL2DZ* optimized structure of **TS1′** with M = Al (**TS1a′**). All bond lengths are in Å.

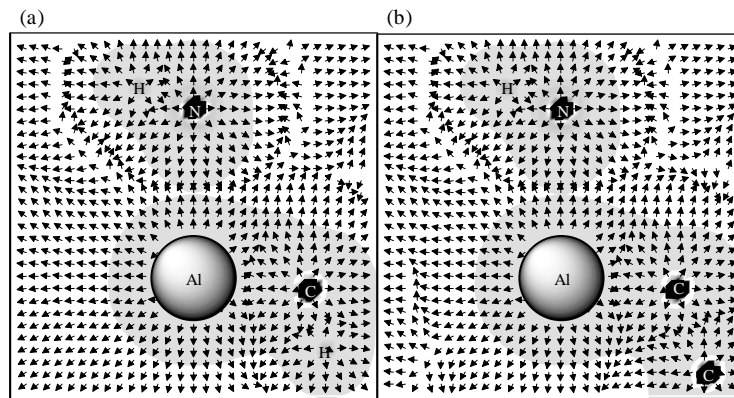Fig. 1. Maps of the kinetic energy density in the σ_v plane for the processes of complex formation: (a) $Al(CH_3)_3$ (**1**) + NH_3 and (b) $Al(C_2H_5)_3$ (**1′**) + NH_3 at 2.95 Å of the Al–N distance. Gray areas are the R_D's where the $n_T(\mathbf{r})$ is positive. Arrows denote the $\vec{\tau}^S(\mathbf{r})$. Circle on Al represents a cross section of pseudopotential with the σ_v plane.

Table 2
Relative energies of RH elimination by unimolecular mechanism at the B3LYP /LanL2DZ* + ZPE level (kcal/mol)

	$R = CH_3$			C_2H_5		
	M = Al	Ga	In	Al	Ga	In
$MR_3 + NH_3$	0.00	0.00	0.00	0.00	0.00	0.00
$R_3M \cdot NH_3$	−20.23	−16.18	−16.08	−18.99	−14.25	−14.30
TS1	7.11	14.26	12.93	6.80	14.56	13.08
$MR_2NH_2 + RH$	−26.32	−22.06	−18.88	−31.31	−23.05	−20.42

found that the difference in the strength of the M–N interaction would affect the activation energy [9–13]. Relation among $M(C_2H_5)_3$ source for the reactivity is same as relation among $M(CH_3)_3$. However, the activation energies of **TS1′** and reaction enthalpies become lower than those of the corresponding system with methyl groups for each M. The cause of fall in the activation energies and reaction enthalpies by substituting ethyl group can be regarded as the stronger M–N interaction in $M(C_2H_5)_3/H_2/NH_3$ system, just as the reactivity with respect to the kind of metal would be controlled by the M–N interaction. Besides, as compared with the complex **2′**, the steric repulsion is reduced to the interference between two ethyl groups in **TS1′** and amide adduct **3′**.

In the presence of excess ammonia, we have found that $M(CH_3)_3$ makes a stable complex due to the coordinate bond with two ammonia molecules, $H_3N \cdot (CH_3)_3M \cdot NH_3$ (**4**), without potential energy barrier [12,13]. Similarly, $M(C_2H_5)_3$ and two ammonia molecule can form a stable complex. Under this condition, the methane/ethane elimination can occur as follows:

$$R_3M \cdot NH_3(2/2') + NH_3 \rightarrow$$
$$H_3N \cdot R_3M \cdot NH_3(4/4'), \qquad (3)$$

$$4/4'[\text{or } 2/2' + NH_3] \rightarrow [TS2/TS2']^{\ddagger} \rightarrow$$
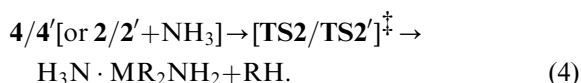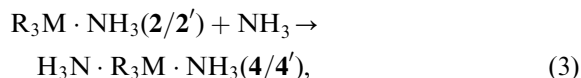$$H_3N \cdot MR_2NH_2 + RH. \qquad (4)$$

Fig. 3 shows the optimized structure of **TS2a′**, and the relative energies of reaction species in reactions (3) and (4) are shown in Table 3. It is found that each of the activation energies of **TS2** and
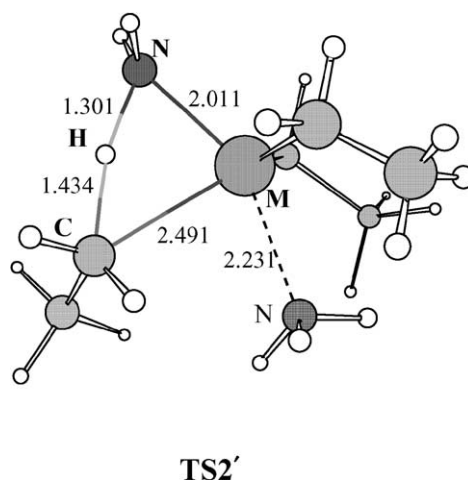

TS2′

Fig. 3. B3LYP/LanL2DZ* optimized structure of **TS2′** with M = Al (**TS2a′**). All bond lengths are in Å.

TS2′ is lower than that of corresponding **TS1** and **TS1′**. Accordingly, in the presence of excess ammonia, the main reaction path of RH molecule elimination is reaction (4) and it is considered that the gas-phase reaction of Al source proceeds more rapidly.

In contrast to **TS1′**, the activation energies of **TS2′** become higher than those of the corresponding **TS2** for each M. Large steric repulsion between ethyl groups and one of ammonia molecules arise by substituting ethyl groups for methyl, and it destabilizes the reaction system more remarkably than steric repulsion in **TS1′**. Practically, ethyl groups would prevent the second ammonia molecule from making a coordinate bond by steric hindrance. It is expected that this

Table 3
Relative energies of RH elimination by unimolecular mechanism in the presence of excess ammonia at the B3LYP/LanL2DZ[*] + ZPE level (kcal/mol)

	R = CH_3			C_2H_5		
	M = Al	Ga	In	Al	Ga	In
$MR + 2NH_3$	0.00	0.00	0.00	0.00	0.00	0.00
$H_3N \cdot R_3M \cdot NH_3$	−24.08	−18.02	−22.48	−22.88	−16.11	−21.18
TS2	4.33	13.88	6.34	5.47	15.42	6.53
$MR_2NH_2 + RH + NH_3$	−26.32	−22.06	−18.88	−31.31	−23.05	−20.42

interference would promote with bulkier alkyl groups.

4. Conclusion

We have discussed the gas-phase parasitic reaction in $MR_3/H_2/NH_3$ system following the elimination of methane or ethane in terms of the regional density functional theory. It is clearly shown that Al source gases enhance reactivity for both of R = CH_3 and C_2H_5. We have demonstrated that the strength of M–N coordination interaction affects the stabilization of the reaction system remarkably. It is found that the substitution of ethyl groups for methyl in metal source builds up the M–N coordination interaction, and essentially the increase in M–N interaction could reduce activation energies of the RH molecule elimination. However, in the presence of excess ammonia, the steric repulsion between ethyl groups and ammonia, which hardly takes place for R = CH_3, raises activation energies. It is considered that the utilization of steric hindrance by bulkier alkyl groups is available method for suppression of the parasitic reaction in the presence of excess ammonia.

Acknowledgements

References

[1] S. Nakamura, Acta Phys. Pol. Sect. A 95 (1999) 153 and references therein.
[2] I. Akasaki, H. Amano, Jpn. J. Appl. Phys. 36 (1997) 5393 and references therein.
[3] K. Uchida, H. Tokunaga, Y. Inashi, N. Akutsu, K. Matsumoto, Mater. Res. Soc. Symp. Proc. 449 (1997) 129.
[4] A. Thon, T.F. Kuech, Appl. Phys. Lett. 69 (1996) 55.
[5] C.H. Chen, H. Liu, D. Steigerwald, W. Imler, C.P. Kuo, M. Ludowise, S. Lester, J. Amano, J. Electron Mater. 25 (1996) 1004.
[6] J.P. Noad, A.J. SpringThorpe, J. Electron Mater. 9 (1980) 601.
[7] S.J. Bass, C. Pickering, M.L. Young, J. Crystallogr. Growth 64 (1983) 68.
[8] C.P. Kuo, J.S. Yuan, R.M. Cohen, J. Dunn, G.B. Stringfellow, Appl. Phys. Lett. 44 (1984) 550.
[9] A. Tachibana, K. Nakamura, O. Makino, H. Tokunaga, N. Akutsu, K. Matsumoto, Blue laser, light emitting diodes, Proceedings of the International Symposium, Ohmsha, Tokyo, 1998, p. 308.
[10] A. Tachibana, O. Makino, S. Tanimura, H. Tokunaga, N. Akutsu, K. Matsumoto, Nitride Semiconductors, Proceedings of the 3rd International Conference, Montpellier, 1999;
A. Tachibana, O. Makino, S. Tanimura, H. Tokunaga, N. Akutsu, K. Matsumoto, Phys. Status Solidi A 176 (1999) 699.
[11] O. Makino, K. Nakamura, A. Tachibana, H. Tokunaga, N. Akutsu, K. Matsumoto, Appl. Surf. Sci. 159–160 (2000) 374.
[12] K. Nakamura, O. Makino, A. Tachibana, K. Matsumoto, J. Organomet. Chem. 611 (2000) 514.
[13] K. Nakamura, O. Makino, A. Tachibana, K. Matsumoto, IPAP Conference Series (Proceedings of the International Workshop on Nitride Semiconductors), Vol. 1, The Institute of Pure and Applied Physics, 2000, p. 97.
[14] K. Nakamura, T. Hayashi, A. Tachibana, K. Matsumoto, J. Crystal Growth 221 (2000) 765.
[15] Molecular Regional DFT Program Package, Tachibana Lab., Kyoto Univ., Kyoto, 2001.

[16] C. Lee, W. Yang, R.G. Parr, Phys. Rev. B 37 (1988) 785.
[17] A.D. Becke, J. Chem. Phys. 98 (1993) 5648.
[18] P.J. Hay, W.R. Wadt, J. Chem. Phys. 82 (1985) 270.
[19] P.J. Hay, W.R. Wadt, J. Chem. Phys. 82 (1985) 299.
[20] T.H. Dunning Jr., P.J. Hay, in: H.F. Schaefer III (Ed.), Modern Theoretical Chemistry, Plenum, New York, 1976.
[21] S. Huzinaga (Ed.), Gaussian basis sets for molecular calculations, Elsevier, New York, 1984, p. 23.
[22] I. Mayer, Int. J. Quantum Chem. 29 (1986) 73, 477
[23] A. Tachibana, Int. J. Quantum Chem. Symp. 21 (1987) 181.
[24] A. Tachibana, R.G. Parr, Int. J. Quantum Chem. 41 (1992) 527.
[25] A. Tachibana, Int. J. Quantum Chem. 57 (1996) 423.
[26] A. Tachibana, Theor. Chem. Acc. 102 (1999) 188.
[27] A. Tachibana, J. Chem. Phys. 115 (2001) 3497.